Theory of nuclear resonant inelastic x-ray scattering from ^{57}Fe in a single-walled carbon nanotube

V. K. Tewary*

Materials Reliability Division, National Institute of Standards and Technology, Boulder, Colorado 80305, USA

A computationally efficient phonon Green's-function method is described for calculation of frequency spectra of single-walled carbon nanotubes containing point defects. The method is generally applicable to defects in other nanostructures. The phonon Green's function is used to calculate line shapes of one-phonon lines in the nuclear resonant inelastic x-ray scattering from ^{57}Fe embedded in a single-walled carbon nanotube. The line shapes are anisotropic and have some unusual features that can provide insight into the physical processes in nanomaterials at atomistic scales and can be used to characterize them. In particular, it may be possible to use the line shapes in certain directions to determine the chirality of a nanotube.

PACS number(s): 81.07.De, 61.72.Bb, 63.22.+m, 76.80.+y

I. INTRODUCTION

We calculate the line shapes of one-phonon lines in the nuclear resonant inelastic x-ray scattering (NRIXS) spectrum from ^{57}Fe in single-walled carbon nanotubes (SWNTs) of different chiralities and diameters using a computationally efficient phonon Green's-function method. We find that the line shapes have unusual features that can provide an insight into the physical processes in SWNTs at the atomistic scale and can be used to characterize them. Similar effects should be observable in the NRIXS spectra of other nanomaterials, particularly nanowires.

Identification of physical processes at the atomistic scale is necessary for characterization of nanomaterials, which is needed for their industrial applications. Conventional methods of characterization of materials that depend on their macroscopic response are not adequate for nanomaterials. We suggest that the nuclear resonance spectroscopy (NRS) can be a valuable tool for quantitatively characterizing the nanomaterials at the atomistic scale. In particular, we show that the NRIXS spectrum in an SWNT is quite sensitive to its chirality as well as diameter. It should be possible, therefore, to use NRIXS to determine the chirality and the diameter of an SWNT.

Chirality is one of the most important parameters of an SWNT, which determines its electronic, optical, and thermal properties.[1] For example, the chirality of an SWNT determines whether it is metallic or semiconducting. Hence, there is a strong industrial and research interest in exploring new physical processes which can be used for measurement of chirality of an SWNT. Chirality of an SWNT can be determined by using transmission electron microscopy but it requires manipulation of individual SWNTs. Chirality can also be obtained from resonance Raman-scattering experiments though the normal Raman scattering gives no information about the chirality.[1] The results of this paper should be useful in developing NRIXS as a spectroscopic method for measurement of chirality and diameter of an SWNT that would supplement other methods of characterizing nanotubes.

NRS and, in particular, NRIXS using the highly brilliant synchrotron radiation are techniques[2–4] that have been found to be very useful for studying phonons and their frequency spectra in solids. The physical process underlying NRS (see Ref. 2 for an excellent review) is very similar to Mössbauer scattering. The scattering of a high-energy photon from a γ isotope embedded in a host solid consists of an elastic part and an inelastic part. The elastic part corresponds to recoilless absorption of a photon, which is the Mössbauer effect. However, the minimum-mass condition[3] for the existence of the recoilless absorption may not be satisfied for an SWNT. The intensity of the Mössbauer line and its second-order Doppler shift depend on the integral of the phonon spectrum of the solid. These quantities, therefore, may not be very sensitive to the details of the phonon spectrum, but may give useful information about the location of the Mössbauer isotope, its binding with the host atoms, and the diameter of the SWNT. Of course, the diameter of an SWNT can be conveniently measured by other methods such as Raman spectroscopy.[1] In this paper, our interest is only in the inelastic scattering.

NRIXS refers to the inelastic scattering of x rays[2,3] from a Mössbauer or a γ isotope that involves exchange of one or more phonons between a photon and the host solid. The line shapes[3] of NRIXS lines depend on the phonon frequency spectrum (density of states) of the solid. The theoretical problem is that the introduction of a γ isotope in a lattice changes its phonon spectrum. Hence, in order to calculate the line shapes, it is necessary to account for the change in the phonon spectrum of an SWNT caused by the introduction of the γ isotope. Moreover, the line shape depends not directly on the phonon spectrum but on the projected phonon spectrum, which is defined in terms of the wave vector of the incident γ photon. Further, as shown in Sec. II B, only the modes close to the impurity atom contribute to the line shape. The NRIXS is therefore sensitive to the local environment of the impurity, which is determined by the chirality of the nanotube.

We derive an expression for the line shape of a one-phonon NRIXS line in an SWNT containing ^{57}Fe in terms of the phonon Green's function[5] that fully accounts for the changes in the phonon spectrum caused by the defect. As an approximation, we have assumed that ^{57}Fe is a substitutional isotopic defect in the SWNT lattice. The effect of this approximation and its validity has been discussed in Sec. III. A

separate detailed calculation is needed to determine a realistic and stable configuration of ^{57}Fe in an SWNT, which would also yield changes in force constants and bond lengths. Once the defect configuration is known, the phonon Green's-function method, as given here, can be applied to model that configuration by redefining the defect space.[5–7]

The Green's-function method is a computationally efficient method for modeling phonons in lattices with and without defects. It has been successfully used for ordinary solids[5–7] but has not yet been applied to nanomaterials. As shown in this paper, the calculation of the phonon spectrum of an SWNT containing a defect is particularly convenient in terms of the phonon Green's function. Knowledge of the phonon spectra of SWNTs (and other nanomaterials) containing defects is essential for calculating their thermodynamic properties and certain electronic and optical properties.[1,8] A real SWNT will always have lattice defects such as vacancies, interstitials, etc., which affect its physical properties.[8] Such defects can be conveniently modeled by using the Green's-function method as described here. The method is also applicable to other nanostructures.

II. THEORY

A. Phonon Green's function for an SWNT

In this section, we present a method for calculating the change in the phonon spectrum of an SWNT due to the presence of a lattice defect by using the phonon Green's-function method. We will also derive expressions for the perfect phonon Green's function (PGF) for an SWNT without any defects and the defect Green's function (DGF) for an SWNT containing a single substitutional lattice defect. The Green's-function method for ordinary three-dimensional (3D) lattices has been described in detail in the classic book by Maradudin *et al.*[5] for phonons and in Ref. [6] for static problems. The Green's-function method has not yet been applied to defects in SWNT lattices. Our method as presented here is an adaptation of the technique given in Refs. [5] and [6] for ordinary solids to nanotubes.

We assume a frame of reference, as shown in Fig. 1. The Z axis is along the cylindrical axis of the SWNT, and the origin of coordinates is at the center of the cylinder. The atoms of the SWNT are located at the cylindrical surface. The X axis is assumed to pass through an atomic site. We will denote the Cartesian components of a vector by the Greek indices α, β, etc., which stand for x, y, or z. Summation over repeated indices is not assumed and will be written explicitly.

We label an atom in the SWNT lattice by a pair of indices $L\kappa$, where L labels a unit cell and κ labels the atom inside a unit cell. The label $L\kappa$ in the SWNT lattice is the same as in the parent graphene lattice. Each unit cell of the SWNT lattice contains two atoms,[1] so $\kappa=0$ or 1. The atom $\kappa=0$ is assumed to be at the origin of the unit cell. The atom on the X axis is labeled as (00), as shown in Fig. 1.

We define the two-dimensional (2D) position vector of an atom $L\kappa$ in the parent graphene lattice with respect to its crystallographic axes as follows:
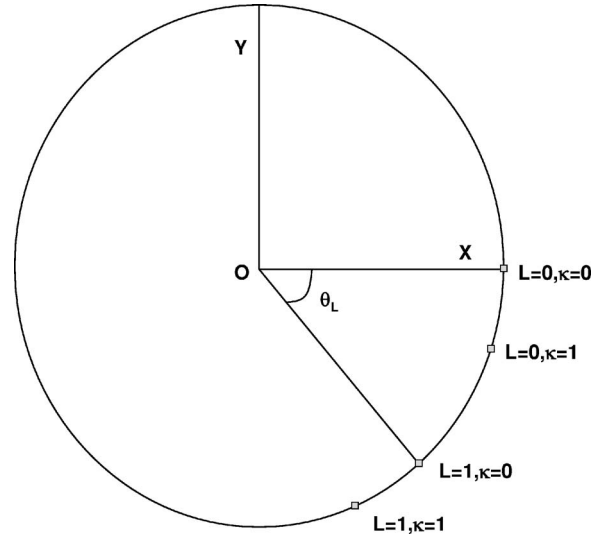

FIG. 1. The frame of reference showing the origin and the X and Y axes for a cylindrical SWNT. The Z axis is along the axis of the cylinder, which is normal to the plane of the paper. All the atoms are located at the surface of the cylinder. The figure shows the locations of atoms in two adjacent unit cells, $L=0$ and $L=1$, each containing two atoms, $\kappa=0$ and $\kappa=1$, and also the angular separation between atoms 00 and 10.

$$\mathbf{R}(L\kappa) = \mathbf{R}(L0) + \mathbf{r}(\kappa), \quad (1)$$

where $\mathbf{r}(\kappa)$ is the position vector of the atom κ with respect to the origin of the unit cell. To avoid any confusion, we emphasize that vectors $\mathbf{R}(L\kappa)$, $\mathbf{R}(L0)$, and $\mathbf{r}(\kappa)$ in Eq. (1) are defined with respect to the crystallographic axes of graphene. Unless otherwise stated, all other expressions in this paper are given in the SWNT frame of reference shown in Fig. 1.

The SWNT lattice is constructed by folding the graphene lattice around the Z axis and along the chiral vector. Hence, the angle $\theta(L\kappa)$ with respect to the X axis subtended by the projection of the atom $L\kappa$ on the chiral vector is given by

$$\theta(L\kappa) = R_C(L\kappa)/R_S, \quad (2)$$

where R_S is the radius of the SWNT and $R_C(L\kappa)$ is the projection of $\mathbf{R}(L\kappa)$ on the chiral vector in the graphene lattice. The SWNT lattice is invariant against a rotation by $\theta(L0)$ about the Z axis. This is equivalent to the translation symmetry of the graphene lattice by the vector $\mathbf{R}(L0)$. The matrix of rotation about the Z axis by an angle $\theta(L\kappa)$ is given by

$$S_Z(L\kappa) = \begin{pmatrix} \cos[\theta(L\kappa)] & -\sin[\theta(L\kappa)] & 0 \\ \sin[\theta(L\kappa)] & \cos[\theta(L)] & 0 \\ 0 & 0 & 1 \end{pmatrix}. \quad (3)$$

We represent the phonons in SWNTs using the Born–von Karman model. The main approximations[5] of this model are (i) adiabatic approximation, (ii) harmonic approximation, and (iii) periodic boundary conditions. We use the fourth neighbor interaction model for the force constants with curvature correction, as described by Saito *et al.*[1] The 3×3 force-constant matrix between two atoms $L\kappa$ and $L'\kappa'$ is denoted by $\phi(L\kappa, L'\kappa')$. If $m(L\kappa)$ denotes the mass and

$\mathbf{u}(L\kappa)$ the 3D displacement of the atom $L\kappa$, we can write the following equation for the atomic displacements:

$$m(L\kappa)\omega^2 u_\alpha(L\kappa) = \sum_{L'\kappa'} \phi_{\alpha\beta}(L\kappa, L'\kappa') u_\beta(L'\kappa'). \quad (4)$$

Equation (4) represents a set of $6N$ homogeneous equations corresponding to three Cartesian coordinates of $2N$ atoms, where N is the total number of unit cells, each containing two atoms. We write Eq. (4) in the form of full-crystal matrices in the vector space of the lattice sites as follows:

$$(\mathbf{M}\omega^2 - \boldsymbol{\phi})\mathbf{u}, \quad (5)$$

where $\boldsymbol{\phi}$ is a $6N \times 6N$ square matrix and $\mathbf{u}$ is a $6N$ dimensional column matrix. Their matrix elements are $\phi_{\alpha\beta}(L\kappa, L'\kappa')$ and $u_\alpha(L\kappa)$, respectively. The matrix $\mathbf{M}$ is a $6N \times 6N$ diagonal matrix of atomic masses. Its matrix elements are as follows:

$$M_{\alpha\beta}(L\kappa, L'\kappa') = m(L\kappa)\delta_K(L\kappa, L'\kappa')\delta_K(\alpha,\beta), \quad (6)$$

where δ_K denotes Kronecker's delta which is unity if its two arguments are equal and zero otherwise. The eigenvalues of the left-hand-side (LHS) matrix in Eq. (5) give the phonon frequencies. There will be $6N$ eigenvalues, some of which may be degenerate.

First, we consider a perfect lattice without defects. For a perfect lattice, $m(L\kappa)$ is independent of L. In the present case of SWNT, the masses of both atoms in the unit cell are the same. So, $m(L\kappa) = m_C$ for all $L\kappa$, where m_C is the mass of a carbon atom. In a normal perfect lattice, which has a translation symmetry, Eq. (5) can be block diagonalized by using the Fourier transform. An SWNT has a helical symmetry[10] about the Z axis. Popov *et al.*[11] have given an elegant transformation that uses the helical symmetry[10] to block diagonalize Eq. (5) for an SWNT. We use a slight variant of this transformation to block diagonalize Eq. (5).

We transform the atomic displacements by using the rotation operator defined in Eq. (3) as follows:

$$\mathbf{v}(L\kappa) = [\mathbf{S}_Z(L\kappa)]^{-1}\mathbf{u}(L\kappa), \quad (7)$$

which transforms Eq. (5) to

$$\boldsymbol{\Lambda}(\omega^2)\mathbf{v} = 0, \quad (8)$$

where

$$\boldsymbol{\Lambda}(\omega^2) = \mathbf{M}\omega^2 - \boldsymbol{\Phi}, \quad (9)$$

and $\boldsymbol{\Phi}$ is the effective force-constant matrix. Its matrix elements are given by

$$\boldsymbol{\Phi}(L\kappa, L'\kappa') = [\mathbf{S}_Z(L\kappa)]^{-1}\boldsymbol{\phi}(L\kappa, L'\kappa')\mathbf{S}_Z(L'\kappa'). \quad (10)$$

Since the lattice is invariant against a rotation by $\theta(L0)$ about the Z axis[10] for any L, $\boldsymbol{\Phi}(L\kappa, L'\kappa')$ will be independent of L and will depend only on the difference of L' and L. We will refer this symmetry as the angular translation symmetry in analogy with the linear translation symmetry exhibited by normal lattices. Equation (5) can be, therefore, block diagonalized by using the Fourier transform over the Brillouin zone of the SWNT, as shown by Popov *et al.*[11] This gives the

following block-diagonalized force-constant matrix in the Fourier space:

$$\Phi^F_{-\alpha\beta}(\kappa, \kappa'; \mathbf{q}) = \sum_{L\kappa'} \Phi_{\alpha\beta}(0\kappa, L\kappa')\exp\{-\iota\mathbf{q}\cdot[\mathbf{R}(L\kappa')$$
$$-\mathbf{R}(0\kappa)]\}, \quad (11)$$

where ι is $\sqrt{(-1)}$ and $\mathbf{q}$ is a 2D wave vector in the Brillouin zone of the graphene lattice.[1,11] The dynamical matrix for phonons is defined by

$$D_{\alpha\beta}(\kappa, \kappa'; \mathbf{q}) = (1/m_C)\Phi^F_{\alpha\beta}(\kappa, \kappa'; \mathbf{q}). \quad (12)$$

The eigenvalues of $\mathbf{D}(\mathbf{q})$ give the phonon frequencies of the perfect SWNT. The matrices $\boldsymbol{\Phi}^F(\mathbf{q})$ and $\mathbf{D}(\mathbf{q})$ are 6×6 and can be diagonalized or inverted numerically. Some authors, as Refs. 1 and 11, define the Fourier transform with respect to the unit-cell coordinates. In Eq. (11), we have defined the Fourier transform with respect to the atomic coordinates as in Ref. 5. This introduces a phase factor in the eigenvectors of $\mathbf{D}$ but does not change its eigenvalues.

The transformed perfect-lattice PGF matrix $\mathbf{G}(\omega^2)$ is defined in the usual way[5,6] as follows:

$$\mathbf{G}(\omega^2) = [\mathbf{M}\omega^2 - \boldsymbol{\Phi}]^{-1}. \quad (13)$$

For a perfect lattice, $\mathbf{M}$ is simply m_C times a unit matrix. By using the orthogonal property of the Fourier transform, we can derive the following expression for the matrix elements of $\mathbf{G}(\omega^2)$ in terms of its Fourier transform from Eqs. (11) and (13).

$$G_{\alpha\beta}(L\kappa, L'\kappa', \omega^2) = (1/N)\sum_q G^F_{\alpha\beta}(\kappa, \kappa'; \mathbf{q}, \omega^2)$$
$$\times\exp\{\iota\mathbf{q}\cdot[\mathbf{R}(L'\kappa') - \mathbf{R}(L\kappa)]\}, \quad (14)$$

where

$$\mathbf{G}^F(\mathbf{q}, \omega^2) = [m_C\omega^2\mathbf{I}_6 - \boldsymbol{\Phi}^F(\mathbf{q})]^{-1}, \quad (15)$$

and $\mathbf{I}_6$ is the 6×6 unit matrix.

The sum in Eq. (14) is over all values of $\mathbf{q}$ in the first Brillouin zone of the SWNT lattice. Since $\boldsymbol{\Phi}^F(\mathbf{q})$ is only a 6×6 matrix, it can be inverted numerically. Equations (14) and (15), therefore, provide a numerically convenient method for calculating the PGF. Before considering the effect of the defect, we will relate the PGF to the phonon frequency spectrum.

The dynamical matrix as defined by Eq. (12) has six eigenvalues for each $\mathbf{q}$, which gives a total of $6N$ phonon frequencies for the lattice corresponding to N allowed values of $\mathbf{q}$. These $6N$ frequencies are the same as the eigenvalues of the LHS matrix in Eq. (5). It is the usual practice to label the phonon frequencies as $\omega(\mathbf{q}j)$, where $j = 1, 2\ldots, 6$ labels the six branches of the dispersion or six eigenvalues of Eq. (12) for each $\mathbf{q}$. For our present purposes, it is more convenient to label all the eigenvalues by a single index s and denote the phonon frequencies by ω_s, where $s = 1, 2\ldots, 6N$.

From Eqs. (11) and (12), we note that the eigenvalues of the $6N \times 6N$ matrix $\mathbf{\Phi}$ are $m_C \omega_s^2$. Using standard matrix algebra, we can write the PGF defined by Eq. (13) in the following form:

$$G_{\alpha\beta}(L\kappa, L'\kappa'; \omega^2) = (1/m_C) \sum_s e_\alpha^S(L\kappa) e_\beta^S(L'\kappa') / (\omega^2 - \omega_S^2),$$

(16)

where $\mathbf{e}^S$ denotes the orthonormalized eigenvector of $\mathbf{\Phi}$ corresponding to the eigenvalue ω_S^2. The spectrum of squared frequencies, that is, the number of frequencies between ω^2 and $d\omega^2$, can be formally written as

$$\gamma(\omega^2) = (1/6N) \sum_S \delta(\omega^2 - \omega_S^2),$$

(17)

where δ denotes the Dirac delta function. The frequency spectrum or the density of states $g(\omega)$ can be related to $\Gamma(\omega^2)$ as follows:

$$g(\omega)d\omega = \gamma(\omega^2)d\omega^2,$$

(18)

which gives

$$g(\omega) = 2\omega\gamma(\omega^2).$$

(19)

Equation (16) shows that the PGF has simple poles on the real axis in the frequency space. Hence, we obtain from from Eqs. (16) and (17)

$$\gamma(\omega^2) = m_C(1/6N\pi)\lim_{\xi \to +0} \text{Im} \sum_{\alpha L\kappa} G_{\alpha\alpha}(L\kappa, L\kappa; \omega^2 - \iota\xi),$$

(20)

where Im denotes the imaginary part. In deriving Eq. (20), we have used the following representation of the delta function:

$$\delta(x) = (1/\pi)\lim_{\xi \to +0} \text{Im } 1/(x - \iota\xi).$$

(21)

Now, we consider the effect of a lattice defect on phonon frequencies and obtain an expression for the defect Green's function. The mathematical formalism is similar to that for ordinary lattices, which has been given in detail in Refs. 5 and 6. Here, we only sketch the technique and describe those features that are specific to the calculation of the DGF for a defect in an SWNT.

The effect of a defect is to change the mass and the force-constant matrices. We denote these changed or the perturbed matrices by $\mathbf{M}^*$ and $\mathbf{\Phi}^*$, respectively, such that

$$\mathbf{M}^* = \mathbf{M} - \Delta\mathbf{M},$$

(22)

and

$$\mathbf{\Phi}^* = \mathbf{\Phi} - \Delta\mathbf{\Phi}.$$

(23)

Using Eqs. (22) and (23) in Eq. (8), we obtain the following eigenvalue equation for the phonon frequencies of the defect lattice:

$$[\mathbf{\Lambda}(\omega^2) - \Delta\mathbf{\Lambda}(\omega^2)]\mathbf{v} = 0,$$

(24)

where

$$\Delta\mathbf{\Lambda}(\omega^2) = \Delta\mathbf{M}\omega^2 - \Delta\mathbf{\Phi}.$$

(25)

From Eq. (24), we obtain

$$[\mathbf{I}_{6N} - \mathbf{G}(\omega^2)\Delta\mathbf{\Lambda}(\omega^2)]\mathbf{v} = 0,$$

(26)

where $\mathbf{I}_{6N}$ is the $6N \times 6N$ unit matrix.

Equation (26) gives the perturbed phonon frequencies which are solutions of the following equation:

$$\Psi(\omega^2) = 0,$$

(27)

where $\Psi(\omega^2)$ is the determinant of $[\mathbf{I}_{6N} - \mathbf{G}(\omega^2)\Delta\mathbf{\Lambda}(\omega^2)]$. The solution of Eq. (27) gives only the frequencies of perturbed modes and not the unperturbed modes.[5] It is apparent from Eq. (26) that these modes are characteristics of the defect represented by $\Delta\mathbf{\Lambda}$ and its coupling with the host atoms represented by $\mathbf{G}$. The new frequencies may lie inside or outside the band of frequencies of the perfect lattice. When they lie within the band, they are called resonance modes[5] and have a wavelike solution. When they lie outside the band, their amplitude decays rapidly with the distance from the impurity and are called localized modes.[5] Their existence depends on the relative change in the mass of the defect and its interaction with the host lattice. If there is no change or only a small change in the force constants, then the localized modes can occur only if the mass of the defect is less than that of the host atoms.

In analogy with the PGF defined by Eq. (13), we define the DGF as follows:

$$\mathbf{G}^*(\omega^2) = [\mathbf{M}^*\omega^2 - \mathbf{\Phi}^*]^{-1} = [\mathbf{\Lambda}(\omega^2) - \Delta\mathbf{\Lambda}(\omega^2)]^{-1}.$$

(28)

In the presence of a defect, $\mathbf{M}^*$ is still diagonal but all its elements are not equal. Similarly, the matrix $\mathbf{\Phi}^*$ does not have the angular translation symmetry. Hence, it is not possible to write $\mathbf{\Phi}^*$ or $\mathbf{G}^*$ in terms of its Fourier transform. Using Eq. (13) in Eq. (28), we can derive the following Dyson equation that gives a relation between $\mathbf{G}^*$ and $\mathbf{G}$:

$$\mathbf{G}^*(\omega^2) = \mathbf{G}(\omega^2) + \mathbf{G}(\omega^2)\Delta\mathbf{\Lambda}(\omega^2)\mathbf{G}^*(\omega^2),$$

(29)

or

$$\mathbf{G}^*(\omega^2) = [\mathbf{I}_{6N} - \mathbf{G}(\omega^2)\Delta\mathbf{\Lambda}(\omega^2)]^{-1}\mathbf{G}(\omega^2).$$

(30)

We see from Eq. (28) that, like the PGF, the DGF has simple poles on the real axis at the eigenvalues of $\mathbf{\Lambda}(\omega^2) - \Delta\mathbf{\Lambda}(\omega^2)$. The DGF, therefore, has contributions from the perturbed mode frequencies given by Eq. (27) as well as the unperturbed modes. Both perturbed and unperturbed modes contribute to the perturbed frequency spectrum of the defect lattice.

Following the steps leading to Eq. (20), we can show that the perturbed spectrum of squared frequencies is given by

$$\gamma^*(\omega^2) = (1/6N\pi)\lim_{\xi \to +0} \text{Im} \sum_{\alpha L\kappa} m(L\kappa)G_{\alpha\alpha}^*(L\kappa, L\kappa; \omega^2 - \iota\xi).$$

(31)

From Eqs. (19), (20), (27), and (31), we obtain[5] the following expression for the change in the phonon spectrum of an SWNT caused by a substitutional lattice defect:

$$\Delta g(\omega) = (1/6N\pi)\lim_{\xi\to+0} \mathrm{Im}\, d/d\omega[\ln \Psi(\omega^2 - \iota\xi)]. \tag{32}$$

The matrices in Eq. (30) and the determinant $\Psi(\omega^2)$ in Eqs. (27) and (30) are all $6N \times 6N$. Since N is usually a large number which may be of the order of several thousands, these equations are not convenient for numerical computations. However, the order of the matrix which actually needs to be inverted in Eq. (30) and that of the determinant which needs to be calculated are substantially reduced in those cases in which $\mathbf{\Delta\Lambda}$ is nonzero only for a finite number of lattice sites. The lattice sites, for which $\mathbf{\Delta\Lambda}$ is nonzero, define a vector space called the defect space. The defect space is obviously a subspace of the vector space of the lattice. If the defect space consists of n lattice sites, the order of the matrix that needs to be inverted in Eq. (30) and the order of $\Psi(\omega^2)$ will be $3n \times 3n$. For example, in the case of an isotopic defect, $n=1$ since an isotopic defect does not involve any changes in the force-constant matrix. In the case the nearest-neighbor force constants are also changed, $n=4$ corresponding to the site containing the defect plus three of its nearest neighbors.

From Eq. (31), we note that $\gamma^*(\omega^2)$ involves sum over the DGF of all the atoms—not just the defect atom. This is of course expected because the frequency spectrum of the whole solid accounts for all the modes of all the atoms in the lattice. Qualitatively speaking, each term on the RHS of Eq. (31) can be visualized as the contribution of the atom $L\kappa$ to the collective vibration modes of the lattice. In the case of a perfect solid, all the atoms in the lattice are equivalent. Hence, each atom contributes equally to the total frequency spectrum. The trace of the PGF in Eq. (20) is therefore simply $2N$ times the term for any atom.

In the case of the DGF in Eq. (31), the translation symmetry is lost and each term is different. Equation (31) is therefore not convenient for numerical calculation of the frequency spectrum of the imperfect lattice. However, the change in the frequency spectrum caused by the defect can be calculated from Eq. (32) since, as described in the preceding paragraph, the determinant $\Psi(\omega^2)$ is only of the order $3n \times 3n$. Only the atoms in the defect space contribute to $\Psi(\omega^2)$. In Sec. II B, we will derive an expression for the line shapes in the NRIXS spectrum of an SWNT containing a γ isotope in terms of the DGF.

B. Calculation of the line shapes in the NRIXS spectra of a γ isotope in an SWNT

We consider a Born–von Karman lattice in thermal equilibrium as described in the preceding section. We calculate the one-phonon scattering cross section of an x-ray photon from a Mössbauer or a γ isotope embedded in an SWNT lattice. As defined by Sturhahn and Kohn,[3] the self-intermediate scattering function S for a photon of wave vector $\mathbf{K}$ is given by

$$S(\mathbf{K},t) = \langle \exp[\iota\mathbf{K} \cdot \mathbf{u}(L\kappa;t)]\exp[-\iota\mathbf{K} \cdot \mathbf{u}(L\kappa;0)]\rangle, \tag{33}$$

where $\mathbf{u}(L\kappa;t)$ is the instantaneous displacement of the atom at $L\kappa$ at time t and angular brackets denote the average over

the canonical ensemble described by the crystal Hamiltonian. In the harmonic approximation, we can express S in terms of the exponent of the displacement correlation function projected on $\mathbf{K}$ and write the cross section $\sigma(\omega)$ for the absorption of a photon from the atom $L\kappa$ that exchanges a phonon of frequency ω in the solid as follows:[9]

$$\sigma(\omega) = (\sigma_0/2)\varepsilon \exp(-2W)\int_{-\infty}^{\infty} dt$$
$$\times \exp(\iota\omega t - \varepsilon|t|)\exp[D_c(\mathbf{K},L\kappa;t)], \tag{34}$$

where

$$D_c(\mathbf{K},L\kappa;t) = \langle \mathbf{K} \cdot \mathbf{u}(L\kappa;t)\mathbf{K} \cdot \mathbf{u}(L\kappa;0)\rangle, \tag{35}$$

where σ_0 is the resonance absorption cross section for the absorbing nucleus, ε is the half-width of the excited state of the nucleus, and $\exp(-2W)$ is the Debye-Waller or the Lamb-Mössbauer factor. A rigorous analysis of $\sigma(\omega)$ has been given in Refs. 2 and 3. Here, we follow the technique given in Ref. 9. By using the normal-mode expansion of the correlation function, its Fourier transform over time can be related[5] to the phonon Green's function $\mathbf{G}^*$ of the lattice as follows:

$$(1/2\pi)\int_{-\infty}^{\infty} dt \exp(\iota\omega t)\langle u_\alpha(L\kappa;t)u_\beta(L\kappa;0)\rangle$$
$$= (\hbar/\pi)\{\mathrm{sgn}(\omega)/[1 - \exp(-\beta_B\hbar\omega)]\}\lim_{\xi\to+0}$$
$$\times \mathrm{Im}\, G_{\alpha\beta}^*(L\kappa,L\kappa,\omega^2 - \iota\xi), \tag{36}$$

where $\beta_B = 1/k_B T$, k_B is the Boltzmann constant, $\hbar$ is Planck's constant divided by 2π, and T is the temperature of the solid. We assume the displacements to be small and expand the exponential of the correlation function in Eq. (34). Keeping only the linear term in the correlation function and using Eq. (36), we obtain the following expression for the cross section for the one-phonon process:

$$\sigma^{(1)}(\omega) = \hbar\sigma_0\gamma \exp(-2W)\{\mathrm{sgn}(\omega)/[1 - \exp(-\beta_B\hbar\omega)]\}\Gamma(\omega), \tag{37}$$

where

$$\Gamma(\omega) = \lim_{\xi\to+0} \Sigma_{\alpha\beta} K_\alpha K_\beta \, \mathrm{Im}\, G_{\alpha\beta}^*(L\kappa,L\kappa,\omega^2 - \iota\xi). \tag{38}$$

The scattering cross section as a function of the phonon frequency ω, as given by Eq. (37), gives the line shape of the one-phonon line. From Eqs. (31) and (38), we observe that the scattering cross section depends on the projected frequency spectrum (projected on the vector $\mathbf{K}$) and not on the frequency spectrum as such that is given by the trace of the Green's-function matrix weighted by the atomic masses. In Eq. (38), depending on the direction of $\mathbf{K}$, the off-diagonal elements of the Green's-function matrix also contribute. This introduces anisotropy in the NRIXS spectra. The frequency spectrum, on the other hand, is not anisotropic. As is apparent from Eqs. (20) and (31), the frequency spectrum is given by the trace of the Green's-function matrix, which averages out the anisotropy.
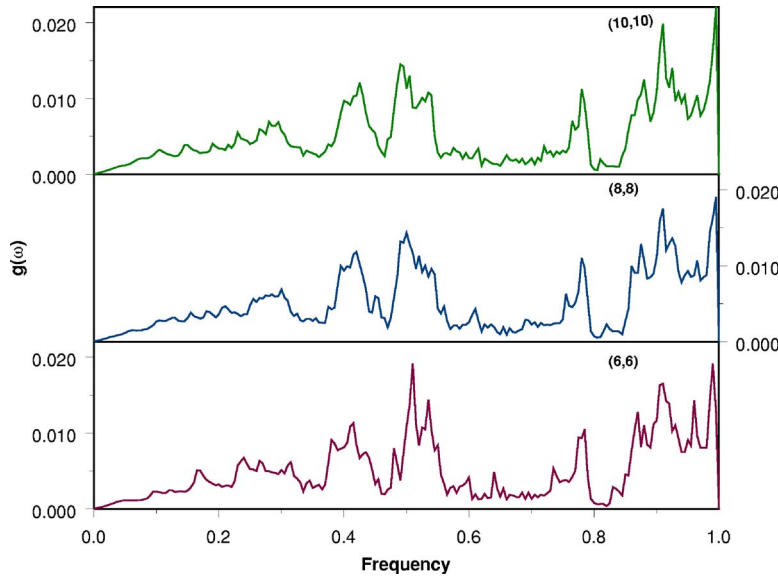
FIG. 2. (Color online) Frequency spectra $g(\omega)$ of perfect SWNTs of similar chiralities but different diameters as function of frequency. The chiral indices and diameters are the following: top panel, (10,10), 34.6; middle panel, (8,8), 27.7; and bottom panel, (6,6), 20.8. The diameters are in units of a/π, where $2a$ is the lattice constant of the SWNT lattice. Functions $g(\omega)$ are normalized such that their integral over the entire frequency range is unity. The frequencies are normalized with respect to the maximum phonon frequency for the SWNT.

Another important point is that the NRIXS line shape does not depend on the total frequency spectrum which is the sum of the Green's-function matrix for all the atoms in the lattice. As we see from Eq. (38), it only depends on the atoms in the defect space. The atoms in the defect space contribute resonance modes to the frequency spectrum and their frequencies depend largely on the local environment of the defect. Only for a perfect lattice, as remarked in the preceding section, the trace of the Green's-function matrix for a single atom gives the total frequency spectrum.

For the qualitative analysis in this paper, our interest is only in the function $\Gamma(\omega)$ that represents the lattice contribution to the line shape. We have used $\mathbf{G}^*$ and not $\mathbf{G}$ in Eq. (36) for the correlation function. It is essential to use the DGF rather than the PGF in Eq. (36) because of the presence of ^{57}Fe in the SWNT which is a lattice defect. Equation (37) is valid only for the band or the resonance modes. The contribution of localized modes,[9] if any, has to be included separately. In the case of ^{57}Fe in an SWNT that we consider in this paper, there will be no localized modes since the mass of ^{57}Fe is much larger than that of ^{12}C.

In the next section, we shall apply the above formulas to calculate the frequency spectra of SWNTs, change in the frequency spectra due to ^{57}Fe impurities in SWNTs, and the line shapes of NRIXS spectra for different SWNTs.

III. RESULTS AND DISCUSSION

First, we consider a perfect SWNT lattice. We assume the most general form of the interatomic force constants extending up to fourth nearest neighbors of each atom including the curvature correction.[1] We use the same numerical values of the force constants as given by Saito *et al.*[1] The geometry of an SWNT is defined in terms of its chirality, which is expressed as the index pair (N,M) in the conventional notation.[1] This should not cause any confusion with our notation N for the number of atoms and $\mathbf{M}$ for the mass matrix because this will be clear from the context and also because the chiral indices (N,M) will always occur in pairs.

We calculate $\mathbf{G}$ from Eqs. (14) and (15) by using the Fourier-transform method. The number of points taken along the Z axis in the Brillouin zone was 80, which was found to be adequate by checking the convergence of the inverse Fourier transform. The frequency spectrum $g(\omega)$ for a perfect SWNT is given by Eqs. (19) and (20). The PGFs are calculated for 1000 frequency intervals in the range $\omega=0-\omega_0$, where ω_0 is the maximum allowed phonon frequency for that SWNT. The value of ξ is taken to be equal to the length of one interval. This value is chosen on the consideration that the numerical integral of the right-hand side (RHS) of Eq. (21) should be close to unity. The frequency spectrum is calculated for 200 frequency intervals in the same range and is obtained by integrating the values of the Green's functions over five frequency intervals. The frequency interval for $g(\omega)$ is chosen to be larger than that for $\mathbf{G}$ in order to avoid too much structure in the curve for reasons of visual clarity. In an actual application, the frequency interval for the calculation of $g(\omega)$ would be determined by the resolution of the measurements.

The calculated values of $g(\omega)$ for different SWNTs have been shown in Figs. 2 and 3 as functions of the normalized frequency $f=\omega/\omega_0$. In each figure, the curves for different (N,M) are shown in different panels in the interest of greater visual clarity. Figure 2 shows $g(\omega)$ for $(N,M)=(6,6)$, (8,8), and (10,10). These SWNTs have similar chirality but their circumferences are 20.8, 27.7, and 34.6, respectively, in units of a, where $2a=2.49$ Å is the lattice constant.[1] We see from this figure that $g(\omega)$ is sensitive to the diameter of an SWNT. The frequency spectrum has only a weak dependence upon chirality, as is apparent from Fig. 3 that shows $g(\omega)$ for $(N,M)=(14,0)$, (10,6), and (8,8). The circumferences of these SWNTs are almost the same being equal to 28, 28, and 27.7, respectively, in units of a, but their chiralities are different.

One important difference between the phonon spectra of an SWNT and a macroscopic solid arises from the fact that the number of allowed wave vectors in the Brillouin zone of an SWNT is much smaller than that in a macroscopic solid.
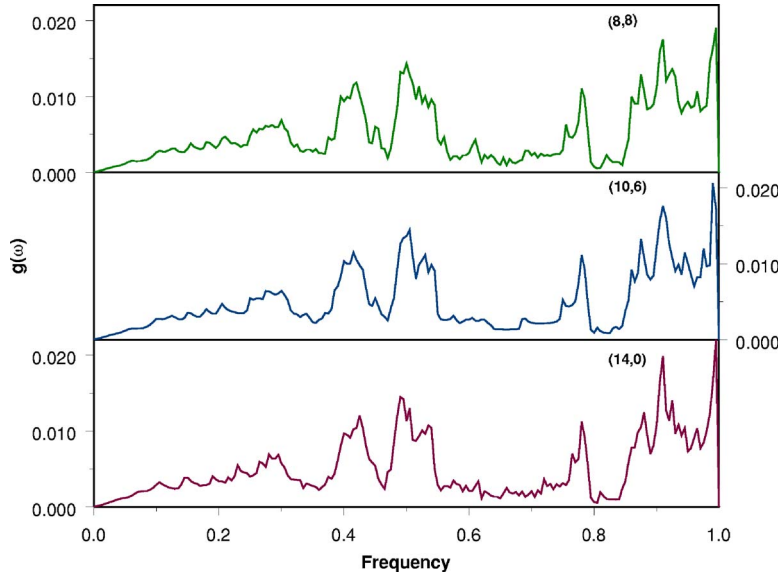
FIG. 3. (Color online) Same as in Fig. 2 for SWNTs of different chiralities but almost equal diameters. The chiral indices and diameters are the following: Top panel, (8,8), 27.7; middle panel, (10,6), 28; and bottom panel, (14,0), 28. The units and normalization are the same as in Fig. 2.

Because a macroscopic solid has a large number of atoms in a supercell (of the order of Avogadro number), the wave vectors in the Brillouin zone are almost continuously distributed. This makes the phonon spectra of macroscopic solids almost continuous. The number of allowed wave vectors in the Brillouin zone of an SWNT is small (10–1000 depending on its chirality) which makes phonon spectrum discrete and gives a lot of structure to the line shape. Moreover, an SWNT, in contrast to ordinary solids, has a 2D lattice structure over a cylindrical surface. The phonon spectrum of a 2D lattice has singularities[5] that are characteristics of the symmetry of the lattice.

Now, we consider an SWNT containing a single ^{57}Fe atom as a point defect. We assume that ^{57}Fe is a substitutional isotopic defect located at 00 in the SWNT lattice. Thus, the ^{12}C atom at 00 is replaced by ^{57}Fe. We will denote the mass of ^{57}Fe by m_D. We further assume that the defect is isotopic which implies that there is no change in the force-constant matrix. Hence, from Eq. (25),

$$\mathbf{\Delta\Lambda}(\omega^2) = \mathbf{\Delta M}\omega^2. \qquad (39)$$

By using Eqs. (6) and (22), the elements of the diagonal matrix $\mathbf{\Delta M}$ can be written as

$$\Delta M_{\alpha\beta}(L\kappa, L'\kappa') = \Delta m\, \delta_K(L\kappa,00)\, \delta_K(L\kappa, L'\kappa')\, \delta_K(\alpha,\beta), \qquad (40)$$

where

$$\Delta m = m_C - m_D. \qquad (41)$$

We see from Eq. (40) that in our assumed defect configuration, $\mathbf{\Delta\Lambda}$ is nonzero only for one lattice site 00. Hence, n for the defect space is 1 and only a 3×3 matrix has to be inverted in Eq. (28). The order of the determinant $\Psi(\omega^2)$ is 3 $\times 3$. Thus, by using the method of matrix partitioning[5,6] in the defect space, we obtain from Eq. (30)

$$\mathbf{G}^*(00,00,\omega^2) = [\mathbf{I}_3 - \Delta m\omega^2\mathbf{G}(00,00,\omega^2)]^{-1}\mathbf{G}(00,00,\omega^2), \qquad (42)$$

and

$$\Psi(\omega^2) = \det[\mathbf{I}_3 - \mathbf{\Delta}m\omega^2\mathbf{G}(00,00,\omega^2)], \qquad (43)$$

where $\mathbf{I}_3$ is the 3×3 unit matrix. All matrices in Eqs. (42) and (43) are 3×3. Since $m_C < m_D$ in the present case, all the phonon frequencies lie within the band of frequencies of the perfect lattice and there are no localized modes.[5]

We calculate $\Delta g(\omega)$ by using Eqs. (32) and (43) for the same SWNTs, as in Figs. 2 and 3. The results are shown in Figs. 4 and 5. The curves have been normalized such that the area under the curve is unity. The normalization factors, denoted by A, used in Figs. 4 and 5 are $A_{10,10}=2.9\times10^{-6}$, $A_{6,6}=9.1\times10^{-5}$, $A_{8,8}=8.5\times10^{-5}$, $A_{14,0}=2.1\times10^{-5}$, and $A_{10,6}=2.9\times10^{-6}$. We see that the magnitude of the change Δg is small compared to the magnitude of g, the perfect-lattice frequency spectrum. Since the total number of modes is $6N$, the change caused by a single impurity atom is expected to be of the order $1/6N$.

We see from Figs. 4 and 5 that $\Delta g(\omega)$ is sensitive to the chirality as well as the diameter of the SWNTs. We also observe that $\Delta g(\omega)$ is 0 at $\omega=0$ and almost 0 for low values of ω. This is physically expected because low frequencies correspond to long-wavelength phonons that are not sensitive to the defect and its local environment. The spectrum in this region $(f<0.1)$ can be approximately represented by the continuum model. The change is more pronounced for larger values of ω. This can be understood by recalling that $g(\omega)$ is the number of frequencies in a certain interval around ω. The function $\Delta g(\omega)$ is not the change in the frequencies but the change in the number of frequencies in that frequency interval. The function $g(\omega)$ is highly oscillatory for larger values of ω and a slight change in frequency of a mode pushes it into a different frequency interval. The vibration frequency of the impurity atom is lower than that of the host atom since it is proportional to the inverse square root of the mass of the
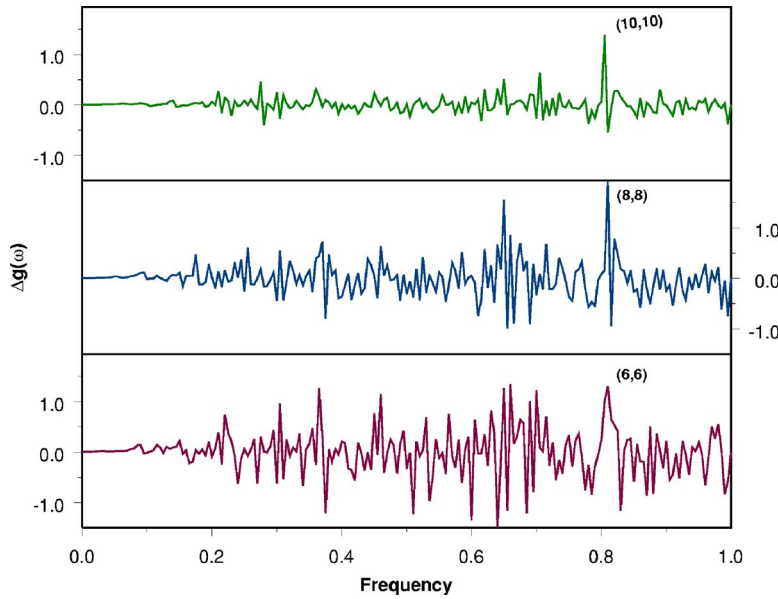
FIG. 4. (Color online) Change in the frequency spectra $\Delta g(\omega)$ due to substitutional ^{57}Fe defects in SWNTs of similar chiralities but different diameters as function of frequency. Functions $\Delta g(\omega)$ are normalized such that their integral over the entire frequency range is unity. Other notations are the same as in Fig. 2.

atom. The actual change in the normal-mode frequencies is, therefore, more in the lower-frequency modes. However, it does not change the frequency spectrum of the whole lattice significantly since the solid behaves like a continuum in the long-wavelength limit.

Finally, we calculate the line-shape function $\Gamma(\omega)$ by using Eqs. (38) and (42) for different values of (N,M) and directions of **K**. The results are shown in Figs. 6–8. In these curves, we have shown $\Gamma(\omega)$ for 1000 frequency intervals over the full frequency range. This is in order to display a detailed structure of the line shape since it is an observable quantity. We have normalized $\Gamma(\omega)$ such that its integral over the entire frequency range is unity. For an SWNT, $\Gamma(\omega)$ is anisotropic and depends on the direction of **K** relative to the axis of the SWNT. Figures 6–8 give the line shapes for **K** along the X, Y, and Z directions, respectively.

We will refer the X direction as the radial direction since it joins the center of the circle with the impurity atom located

at the circumference. A perfect SWNT, of course, has a radial symmetry in which the X and Y directions are equivalent. In the present case, the radial symmetry is violated because the impurity atom is located on the X axis. This introduces anisotropy in the NRIXS spectrum, which should be observable because the spectra in different directions should be different. Experimentally, it is perhaps not possible to observe the exact location of the defect on the surface of the SWNT. However, if the spectra are observed in different directions on the plane normal to the axis of the SWNT, the difference in the spectra should show the anisotropy and give useful information about the chirality of the SWNT as well as the location of the defect.

As physically expected, the line shape for **K** along the radial direction (X axis) is not sensitive to the chirality but is sensitive to the diameter of the SWNT. Its dependence on chirality is, therefore, not shown here. Figure 6 shows the line shapes for $(N,M)=(6,6)$, $(8,8)$, and $(10,10)$, which have similar chirality but their diameters are different. The line
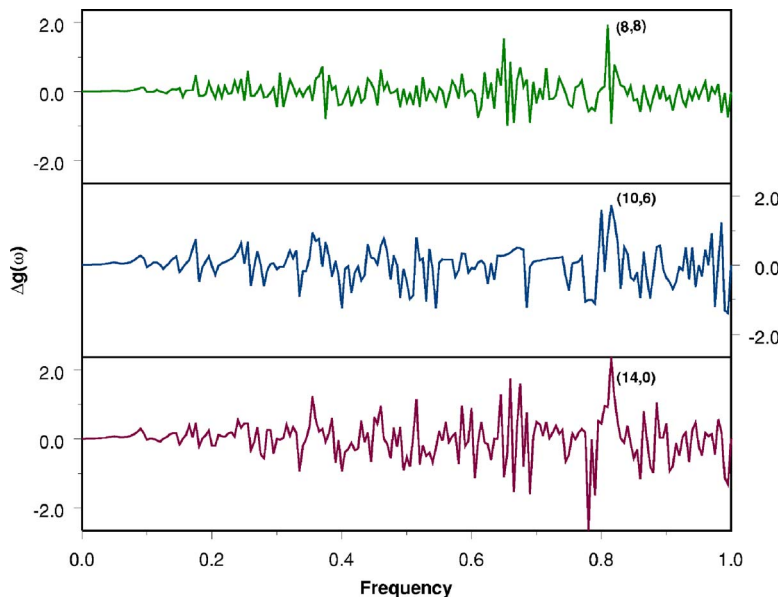

FIG. 5. (Color online) Same as in Fig. 4 for SWNTs of different chiralities but almost equal diameters. Chiral indices and diameters are the same as in Fig. 3.
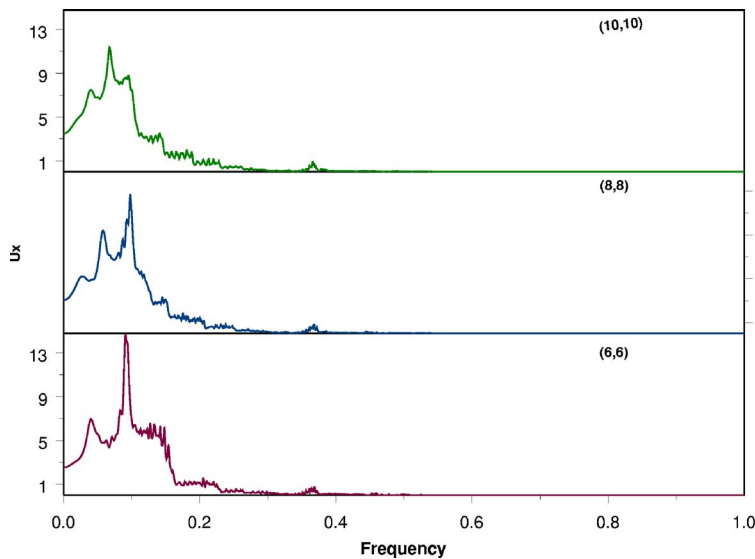
FIG. 6. (Color online) Dependence of the line shape U_X of the one-phonon NRIXS line in the radial direction (X direction in Fig. 1) on the diameter of SWNTs with similar chiralities. Line shapes are normalized such that their integral over the entire frequency range is unity. Other notations are the same as in Fig. 2.

shapes in the Y and Z directions are quite sensitive to chirality. These results are shown in Figs. 7 and 8 for $(N,M) = (10,6)$, $(14,0)$, and $(8,8)$ which have about the same diameter. The distinguishing features in the line shapes are the number of peaks, their positions, and their relative heights. The line shapes in the Y and Z directions also depend on the diameter of the SWNT. This dependence is similar to that in the radial direction and is not shown here.

The number and density of the peaks in the line shape are characteristics of the chirality of the SWNT. Peaks in the line shape occur at the poles of the Green's function, which correspond to the resonance modes induced by the defect as well as the discrete unperturbed frequencies of host lattice. The discrete phonon frequencies are located at the allowed discrete values of the angular wave vector in the Brillouin zone, which, for an SWNT, is determined by its chirality.[1] The number of allowed angular wave vectors is smaller for SWNTs having higher symmetries as for $N=M$ or $M=0$ as compared to those with lower symmetries. For example, this number is 16 for $(8,8)$, 20 for $(10,10)$, 28 for $(14,0)$, and 196 for $(10,6)$. When the number of peaks is large in a frequency

interval, their density may become too large to resolve. Then, the line-shape curve will be averaged out and appear to be smooth in that region. This is apparent in the curves for $(10,6)$ in Figs. 7 and 8. Thus, the number and the density of the peaks in the line-shape function are identifiers for the chirality of the SWNTs. In practice, it may be more convenient to analyze the observed line-shape function in terms of its Fourier transform or moments.

As discussed in the preceding section, the NRIXS spectrum does not depend on the total frequency spectrum but depends on the modes in which the impurity atom vibrates and would include resonance modes. The dependence on chirality arises from the coupling between the modes. This is reflected in Figs. 6–8. We note from Figs. 6–8 that the peaks occur at the lower end of the spectrum, that is, for $f < 0.5$. This is expected because the impurity atom ^{57}Fe is about 4.75 times heavier than the host ^{12}C. A crude estimate of the change in frequencies can be made as follows. For uncoupled atoms, the vibration frequency varies as inverse square root of the mass. So, the vibration frequency of an uncoupled ^{57}Fe will be about $1/\sqrt{4.75} = 0.46$ times that of C. This estimate is consistent with the behavior of the curves in
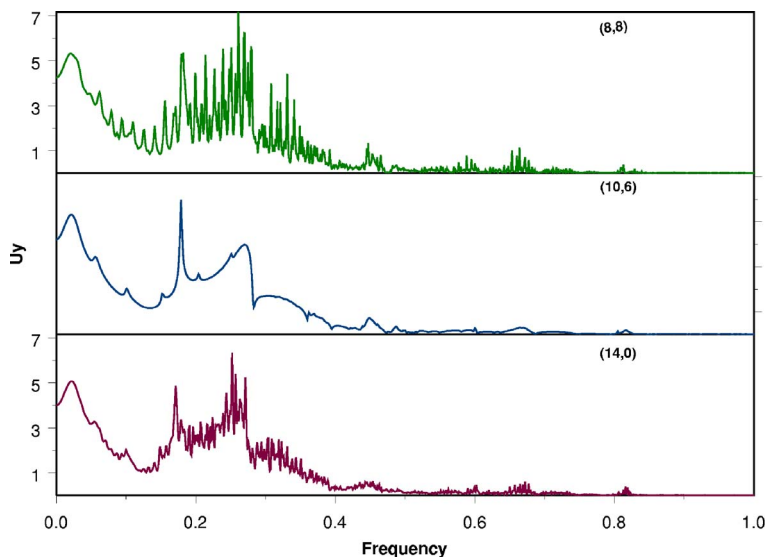

FIG. 7. (Color online) Dependence of the line shape U_Y of the one-phonon NRIXS line in the Y direction on the chirality of SWNTs with almost equal diameters. Chiral indices and diameters, same as in Fig. 3. Normalization as described in Fig. 6.
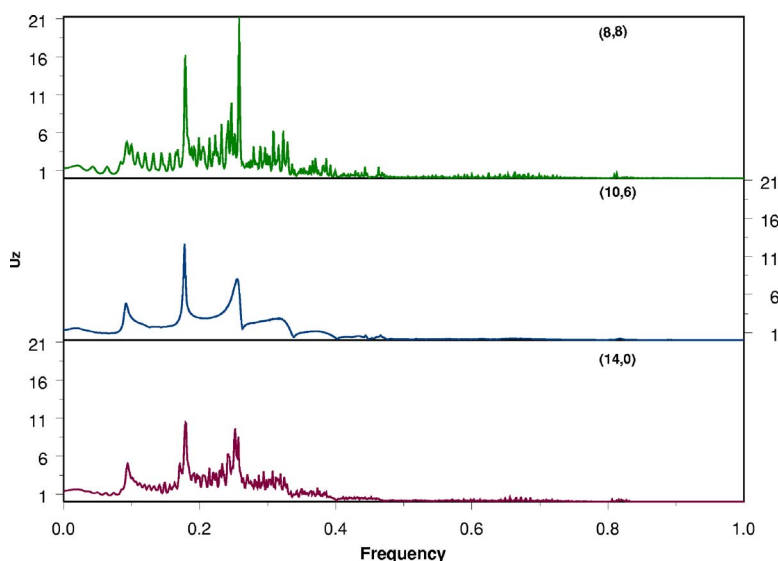
FIG. 8. (Color online) Same as Fig. 7 but in the axial direction (Z direction) of the SWNTs.

Figs. 6–8 since all the peaks occur for $f < 0.5$ of the maximum frequency. It is interesting to note that the NRIXS picks up low frequencies even in the region $f < 0.1$ which would not show up in the total frequency spectrum because they get smeared out in the continuum.

We have made a rather crude approximation that the defect does not change the interatomic force constants. However, our results should be at least qualitatively reliable because a change in force constants is qualitatively equivalent to a change in the effective mass of the impurity. If the binding between the impurity and the host is stronger, its effective mass will be reduced and the peaks in the line-shape function will shift toward the higher end of the spectrum. We have not included the effect of other point defects such as vacancies, self-interstitials, etc., which would normally be present in real SWNTs and will affect the frequency spectra and the line shape. However, because the mass of Fe is much larger than the effective mass of the vacancy and the self-interstitials, its effect is likely to dominate over the changes in the phonon spectra induced by other defects, particularly at low frequencies.

Another major approximation in this paper is that we have assumed the defect to be substitutional. In a real case, the defect may be attached to a C atom and located off the surface of the nanotube. This case may also be qualitatively modeled by assuming a heavier substitutional defect of mass equal to the combined mass of Fe and C atoms. This will result into a further shift toward the lower-frequency end of the phonon spectrum. It would require a detailed molecular-dynamics or *ab initio* calculation to determine the exact location of the defect. If the location of the defect is known theoretically, the NRIXS line shapes can be calculated by using the Green's-function method described in this paper.

Alternatively, an experimental study of NRIXS or NRS spectra can yield information about the location of the defect.

To summarize, this paper makes two contributions: A phonon Green's-function method for calculation of change in the phonon spectrum of an SWNT due to a lattice defect and a theoretical analysis of the NRIXS spectra of ^{57}Fe in SWNTs. We have calculated the line shape of one-phonon lines in the NRIXS spectra of ^{57}Fe in SWNTs of different chiralities and diameters. We show that the NRIXS can yield useful information about the chirality, diameter, and orientation of an SWNT.

An important feature of NRIXS (Ref. 2) is that only the Mössbauer isotope contributes to the signal and the nonactive material does not contribute any background noise. So, if an active SWNT (the one containing the Mössbauer isotope) is part of a bundle of randomly oriented nonactive SWNTs, it can be examined by NRIXS without the spectrum being clouded by the nonactive SWNTs in the bundle.

A more detailed theory will be needed for a quantitative interpretation of the experimental data and actual determination of chirality and other parameters of an SWNT from the observed NRIXS data. We hope this work will inspire more theoretical and experimental work to explore the use of NRS, in particular, NRIXS, for characterization of SWNTs and other nanostructures, particularly nanowires. Our results should be useful in designing such experiments and for their qualitative interpretation.

*Electronic address: tewary@boulder.nist.gov

[1] R. Saito, G. Dresselhaus, and M. S. Dresselhaus, *Physical Properties of Carbon Nanotubes* (Imperial College Press, London, 2004).

[2] W. Sturhahn, J. Phys.: Condens. Matter **16**, S497 (2004).

[3] W. Sturhahn and V. G. Kohn, Hyperfine Interact. **123/124**, 367 (1999).

[4] Y. Q. Cheng, S. Y. Zhou, and B. F. Zhu, Phys. Rev. B **72**, 035410

(2005).

[5] A. A. Maradudin, E. W. Montroll, G. H. Weiss, and I. P. Ipatova, in *Theory of Lattice Dynamics in the Harmonic Approximation*, Solid State Physics Suppl. 3, 2nd ed., edited by H. Ehrenreich, F. Seitz, and D. Turnbull (Academic, New York, 1971).

[6] V. K. Tewary, Adv. Phys. **22**, 757 (1973).

[7] V. K. Tewary, Phys. Rev. B **66**, 205321 (2002).

[8] H. Paulsen, H. Winkler, A. X. Trautwein, H. Grünsteudel, V. Rusanov, and H. Toftlund, Phys. Rev. B **59**, 975 (1999).

[9] A. A. Maradudin, Solid State Phys. **18**, 274 (1966).

[10] C. T. White, D. H. Robertson, and J. W. Mintmire, Phys. Rev. B **47**, 5485 (1993).

[11] V. N. Popov, V. E. Van Doren, and M. Balkanski, Phys. Rev. B **61**, 3078 (2000).